Available online at www.sciencedirect.com
ScienceDirect
Progress in Natural Science 18 (2008) 71–78
Progress in Natural Science

Influence of mesoscale topography on vortex intensity

Zhexian Luo *, Yun Gao

Remote Sensing College, Nanjing University of Information Science and Technology, Najing 210044, China

Received 16 March 2007; received in revised form 8 May 2007; accepted 8 June 2007

Abstract

The effect of mesoscale topography on multi-vortex self-organization is investigated numerically in this paper using a barotropic primitive equation model with topographic term. In the initial field there are one DeMaria major vortex with the maximum wind radius r_m of 80 km at the center of the computational domain, and four meso-β vortices in the vicinity of r_m to the east of the major vortex center. When there is no topography present, the initial vortices self-organize into a quasi-final state flow pattern, i.e. a quasi-axisymmetric vortex whose intensity is close to that of the initial major vortex. However, when a mesoscale topography is incorporated, the spatial scale of the quasi-final state vortex reduces, and the relative vorticity at the center of the vortex and the local maximum wind speed remarkably increase. The possible mechanism for the enhancement of the quasi-final state vortex might be that the negative relative vorticity lump, generated above the mesoscale topography because of the constraint of absolute vorticity conservation, squeezes the center of positive vorticity towards the mountain slope area, and thus reduces the spatial range of the major vortex. Meanwhile, because the total kinetic energy is basically conservative, the squeezing directly leads to the concentration of the energy in a smaller area, i.e. the strengthening of the vortex.

Keywords: Mesoscale topography; Vortex; Self-organization; Intensity change

1. Introduction

The effect of topography on the structure, track, and intensity of vortex is an important topic in vortex dynamics, and a series of relevant results have been presented. When a typhoon vortex approaches the Taiwan island from the east, a new positive vorticity center is generated to the west of the island and structural change of the vortex from single-center vortex to double-center one happens frequently [1–3]. Luo and Chen [4] investigated the effect of terrain on the propagation of vortex Rossby waves, and found that terrain may change the asymmetric structure of the pressure field of typhoon vortex. And terrain may also deflect the track of vortex [5–7]. Based on synoptic studies, Chen and Ding [1] pointed out that when a vortex lies on the windward slope of mountains, the enhancement of the ascending motion can result in a strengthening of the vortex, and that almost every torrential rain associated with typhoons is related with terrain. Smolarkiewice and Rotunno [8] studied lee waves and lee vortices when the air flow passed over a ball-shaped mountain under the condition that Froude number F_r is 0.5. Recently, the studies of the lee wave and lee vortex have obtained great achievements. Gao et al. [9,10] investigated the effect of Tibetan plateau on the flow passing over Tibet. Gao et al. [11] discovered that for the formation mechanism of the lee vortex, there are obvious differences in the rotating case compared with the non-rotating case.

In recent years, self-organization has become a topic of interest in many fields. Self-organization provides a novel path of analyses, and in this paper a possible mechanism for the effect of terrain on the intensity of vortex is going to be analyzed by way of vortex self-organization.

* Corresponding author. Fax: +86 25 58731191.
E-mail address: Luozxma@Yeah.net (Z.X. Luo).

1002-0071/$ - see front matter
doi:10.1016/j.pnsc.2007.06.001

Enagonio and Montgomery [12] set one major vortex of typhoon scale in the initial field and four meso-β vortices in the vicinity of the maximum wind radius to the east of the major vortex. Through self-organization the major vortex absorbed the four meso-β vortices, resulting in a final state flow pattern, i.e. an axisymmetric vortex. And during the evolution process of the vortices without background flow, the intensity of the major vortex changed. Luo and Liu [13] analyzed the interaction of a major vortex with meso-β scale vortices embedded in the horizontal shearing currents, and pointed out that the incorporation of horizontally shearing enhances the intensity of final state self-organized vortex. Based on the studies of Enagonio et al. [12] and Luo et al. [13], in this paper, the multi-vortex self-organization in an ambient horizontally shearing flow above the underlying surface of a mesoscale topography and the topographic effect on the intensity of self-organized major vortex are further investigated.

2. Model and experiment design

2.1. The shallow water primitive equation model

The numerical model used for this work is a shallow water primitive equation model in Cartesian coordinates (x, y) with a uniform resting depth, similar to Evans et al. [14]. Spatial differencing adopts the mean enstrophy and mean kinetic energy conserving scheme of Arakawa and Lamb, which uses the flux form of the shallow water equations on an Arakawa C-grid. The complete prognostic equations are

$$\frac{\partial u}{\partial t} - v^* q + \frac{\partial}{\partial x}(k+p) = 0 \tag{1}$$

$$\frac{\partial v}{\partial t} + u^* q + \frac{\partial}{\partial y}(k+p) = 0 \tag{2}$$

$$\frac{\partial h}{\partial t} + \frac{\partial u^*}{\partial x} + \frac{\partial v^*}{\partial y} - \frac{\partial u_b^*}{\partial x} - \frac{\partial v_b^*}{\partial y} = 0. \tag{3}$$

Here u is the east–west zonal velocity, v is the north–south meridional velocity, $P = gh$ is the geopotential, g is the gravitational acceleration, and h is the depth of the fluid; $u^* = hu$ and $v^* = hv$, and $k = (u^2 + v^2)/2$; the potential vorticity q is given by $q = (\partial v/\partial x - \partial u/\partial y + f)/h$, where f is the Coriolis parameter; $u_b^* = h_b u, v_b^* = h_b v$, where h_b is the height of the topography given by

$$h_b = \begin{cases} h_o \cos(r_b \pi / r_s), & r_b < r_s, \\ 0, & r_b \geqslant r_s, \end{cases} \tag{4}$$

where $r_b = \sqrt{(x - x_h)^2 + (y - y_h)^2}$, and ($x_h$, y_h) is the position of topography center. A resting fluid depth of 5 km is chosen to give a maximum gravity wave speed of approximately 224 $m \cdot s^{-1}$.

The model domain is 2000 km × 2000 km with a grid resolution of 5 km. Asselin time stepping is used and our simulations use a time step of 2.5 s. Five-point spatial smoothing is performed every 10-model minutes.

2.2. Boundary conditions

Cyclic boundaries are prescribed to the east and west. At the north and south boundaries, set

$$\frac{\partial u}{\partial t} + \frac{\partial}{\partial x}(k+P) = 0,$$
$$\frac{\partial h}{\partial t} + \frac{\partial u^*}{\partial x} = 0.$$

To prevent gravity waves reflected at the edges of the domain from propagating back into the vortical area, a simple sponge ring is employed. The computational formula is as follows (taking the west boundary as an example):

$$\widehat{F}_{i,j} = (1 - \alpha_i) F_{i,j} + \alpha_i F_{1,j}, \tag{5}$$

where $\widehat{F}_{i,j}$ is the value on correction using the sponge boundary condition, α_i is the corrective coefficient, $F_{i,j}$ is the predictive value before correcting, with $i = 1,2,\ldots,10$, $F_{1,j}$ is the predictive value at the west boundary. The sponge range covers 50-km in width. α_1, α_2, α_{10} are set to be 1.00, 0.80, 0.60, 0.45, 0.30, 0.20, 0.15, 0.10, 0.05, 0.00, respectively.

2.3. Initial conditions

Set

$$h(x,y,0) = h_{T\beta}(x,y,0) + h_s(y,0) + H \tag{6}$$

at $t = 0$, where $h_{T\beta}$ stands for the sum of the initial basic-state circular vortex and anomaly in terms of the height field, h_s denotes the height field of the subtropical high ridge, and H the resting fluid depth.

The initial basic-state circular vortex employed here is defined [15] as

$$v_{bs}(r) = 2V_m(r/r_m)(1/(1 + (r/r_m)^2)) \exp(-a(r/r_m)^b), \tag{7}$$

where v_{bs} is the azimuthal mean tangential wind velocity, r is the radial distance from the center of the vortex, and V_m, r_m, a, and b are constants, with $V_m = 5$ ms^{-1}, $r_m = 80$ km, $a = 5.5 \times 10^{-6}$, and $b = 6$ [16].

From $V_{bs}(r)$ we can work out $u_{bs}(x,y,0)$, $v_{bs}(x,y,0)$, and $\xi_{bs}(x,y,0)$ at every grid point of the computational domain with ξ_{bs} as the relative vorticity of the basic-state circular vortex.

We assume that there are four-cluster anomalies. The anomalies are given by [12]

$$\xi' = \begin{cases} \xi'_{max} \sum\limits_{i=1,4} \sin^2(\pi(\delta r_i - \Delta)/2\Delta), & \delta r_i < \Delta \\ 0, & \delta r_i \geqslant \Delta. \end{cases} \tag{8}$$

Here δr_1, δr_2, δr_3 and δr_4 are the distances from the anomaly centers (x_{d1}, y_{d1}), (x_{d2}, y_{d2}), (x_{d3}, y_{d3}), and (x_{d4}, y_{d4}), respectively; ξ'_{max} and Δ are parameters describing the amplitude and width of the anomalies, respectively; $\xi'_{max} = 1.74 \times 10^{-4}$ s^{-1}, $\Delta = 50$ km, (x_{d1}, y_{d1}) = (500) km, (x_{d2}, y_{d2}) = (100, −50) km, (x_{d3}, y_{d3}) = (1500) km, (x_{d4}, y_{d4}) = (100,50) km, $g = 9.8 m \cdot s^{-2}$.

ψ' can be worked out from ξ' by the successive overrelaxation, and $\hat{\xi}' = \nabla^2\psi'$ and the difference $\Delta\xi' = \xi' - \hat{\xi}'$. The maximum of $\Delta\xi'/\xi'$ is smaller than 0.1%. u' and v' are then calculated via $\boldsymbol{Z}\times\nabla\psi'$, where $\boldsymbol{Z}$ is the vertical unit vector, and added to the basic-state winds to get $\tilde{u} = u_{bs} + u'$ and $\tilde{v} = v_{bs} + v'$.

In cases where a balanced height field is desired, a successive overrelaxation for

$$\nabla^2 h_{T\beta} = (1/g)\left(f\xi + 2\left(\frac{\partial\tilde{v}}{\partial y}\frac{\partial\tilde{u}}{\partial x} - \frac{\partial\tilde{v}}{\partial x}\frac{\partial\tilde{u}}{\partial y}\right)\right) \tag{9}$$

is performed to calculate $h_{T\beta}(x, y, 0)$ in (6). The tolerance required for $h_{T\beta}$ is $\left(g\nabla^2 h_{T\beta} - (f\zeta + 2(\partial\tilde{v}/\partial y)(\partial\tilde{u}/\partial x) - (\partial\tilde{v}/\partial x)(\partial\tilde{u}/\partial y))\right)_{max} < 0.001/f\xi$. $h_s(y, 0)$ in (6) is determined by [14]

$$h_s(y,0) = -\left(\frac{fh_{s0}}{f_0}\sin\frac{2\pi y}{w}\right) - \frac{\beta h_{s0} w}{2\pi f_0}\cos\left(\frac{2\pi y}{w}\right). \tag{10}$$

Here $f = 2\Omega\sin\varphi$, and $f_0 = 2\Omega\sin\varphi_0$, where φ_0 is the latitude for the middle line of the computational domain with $\varphi_0 = 20°N$; h_{s0} is the parameter for intensity; w is the distance between the north and south boundaries of the computational domain, with $w = 2000$ km; $\beta = (2\Omega/\tilde{a}\cos)\varphi$, where $\tilde{a}$ is the radius of the earth.

$u_s(y, 0)$ and $v_s(y, 0)$ can be worked out from $h_s(y, 0)$ according to the geostrophic balance relation, and adding $u_s(y, 0)$ to $\tilde{u}(x, y, 0)$, we can obtain the initial zonal velocity field, $\tilde{v}(x, y, 0)$, simply used as the initial meridional velocity field. The initial height field can be worked out by substituting $h_{T\beta}(x, y, 0)$ and $h_s(y, 0)$ into (6). The Nitta-Hovermale dynamic initialization scheme is adopted in this study.

2.4. Experiment design

Experiment A (EXA): $h_0 = 0$, without topography; Experiment B (EXB): $h_0 = 4000$ m, with topography. Comparing EXA with EXB, we can analyze the effect of topography on the self-organization of multi-vortices.

3. Major results

3.1. Effect of topography on the axisymmetrization of the major vortex

The temporal evolution of the relative vorticity field in EXA (without terrain) during 0–7 h is shown in Fig. 1.

The following evolution process can be seen from Fig. 1: when $t = 0$ h, in the initial field there are four meso-β scale vortices at about r_m to the east of the major vortex center (Fig. 1(a)), and it is a typically non-axisymmetric flow pattern. Because meso-β scale vortices are embedded in the anticlockwise rotation basic flow of the major vortex, they shift anticlockwise after integration starts (Fig. 1(a)–(h)). Among the four initial meso-β scale vortices, the initial west vortex gradually merges into the major vortex, and the initial north vortex gradually approaches the major vortex, and has been connected with the major vortex after $t = 6$ h. The initial east and south vortices still exist at $t = 7$ h.

After 7 h (Fig. 2), they gradually merge into the major vortex, resulting in a quasi-axisymmetric flow pattern at $t = 36$ h. This quasi-final state flow pattern consists of two parts, i.e. an inner region and an outer region of spiral-band shape. Obviously, this is a typhoon-like vortex (Fig. 2).

The temporal evolution of the relative vorticity field in EXB (with terrain) during 0–7 h is displayed in Fig. 3.

The anticlockwise shift of meso-β scale vortices and the complete mergence of the initial west meso-β scale vortex with the major vortex in EXA still exist in experiment B (Fig. 3(a)–(h)), and after 7 h the four initial meso-β scale vortices are also all absorbed by the major vortex (Fig. 4).

The main difference of EXA from EXB is that their axisymmetrization processes have different charicteristics. As is well known, the axisymmetric flow pattern of vortex must satisfy two conditions. First, contours exhibit an almost circle shape, and second, the center of vortex lies in the vicinity of the center of the circle. The flow patterns at $t = 28$ h, 32 h, and 36 h in EXA (Fig. 2(f)–(h)) basically satisfy the above two conditions. However, those at $t = 28$ h, 32 h, and 36 h in EXB (Fig. 4(f)–(h)) are far different from the two conditions.

It can be seen from the above-mentioned results that when there is no terrain present, the initial non-axisymmetric flow pattern of the coexistence of five vortices, through self-organization, may evolve to a quasi-axisymmetric typhoon-like vortex, but when a mesoscale topography is incorporated into the model, this quasi-axisymmetric quasi-final state flow pattern does not form.

3.2. Effect of topography on the intensity of major vortex

The relative vorticity at the center of vortex ξ_{max} is generally used to represent the intensity of the vortex. The outmost contours of relative vorticity in Figs. 1–4 denote $\xi = 0.5\times10^{-4}\ s^{-1}$, and the contour interval is $0.5\times10^{-4}\ s^{-1}$.

In EXA, ξ_{max} remains stable, at about $3.0\times10^{-4}\ s^{-1}$ throughout the whole integration period of 36 h (Figs. 1 and 2). However, in EXB, it temporally oscillates around a general increasing trend. That is to say, $\xi_{max} = 3.0\times10^{-4}\ s^{-1}$ when $t = 0$ h (Fig. 3(a)), $\xi_{max} = 2.5\times10^{-4}\ s^{-1}$ during $t = 1$–2 h (Fig. 3(b)–(c)), ξ_{max} increases from $3.0\times10^{-4}\ s^{-1}$ to $5.0\times10^{-4}\ s^{-1}$ during $t = 3$–12 h (Fig. 3(d)–(h), Fig. 4(a)–(b)), then reduces to 4.0×10^{-4}–$4.5\times10^{-4}\ s^{-1}$ again in $t = 16$–20 h (Fig. 4(c)–(d)), reaches the maximum value of $6.0\times10^{-4}\ s^{-1}$(twice the initial value of $3.0\times10^{-4}\ s^{-1}$) in the period of $t = 24$–28 h (Fig. 4(e)–(f)), and then slightly declines in $t = 32$–36 h (Fig. 4(g)–(h)).

The maximum wind speed of vortex is another quantity indicating the intensity of vortex. The local maximum wind speed V_{max} in EXA reduces slightly with time (Fig. 5). The smoothing is generally employed to deal with the nonlinear instability in numerical integration of model, and in fact this is equivalent to adding a dissipative term, which accounts

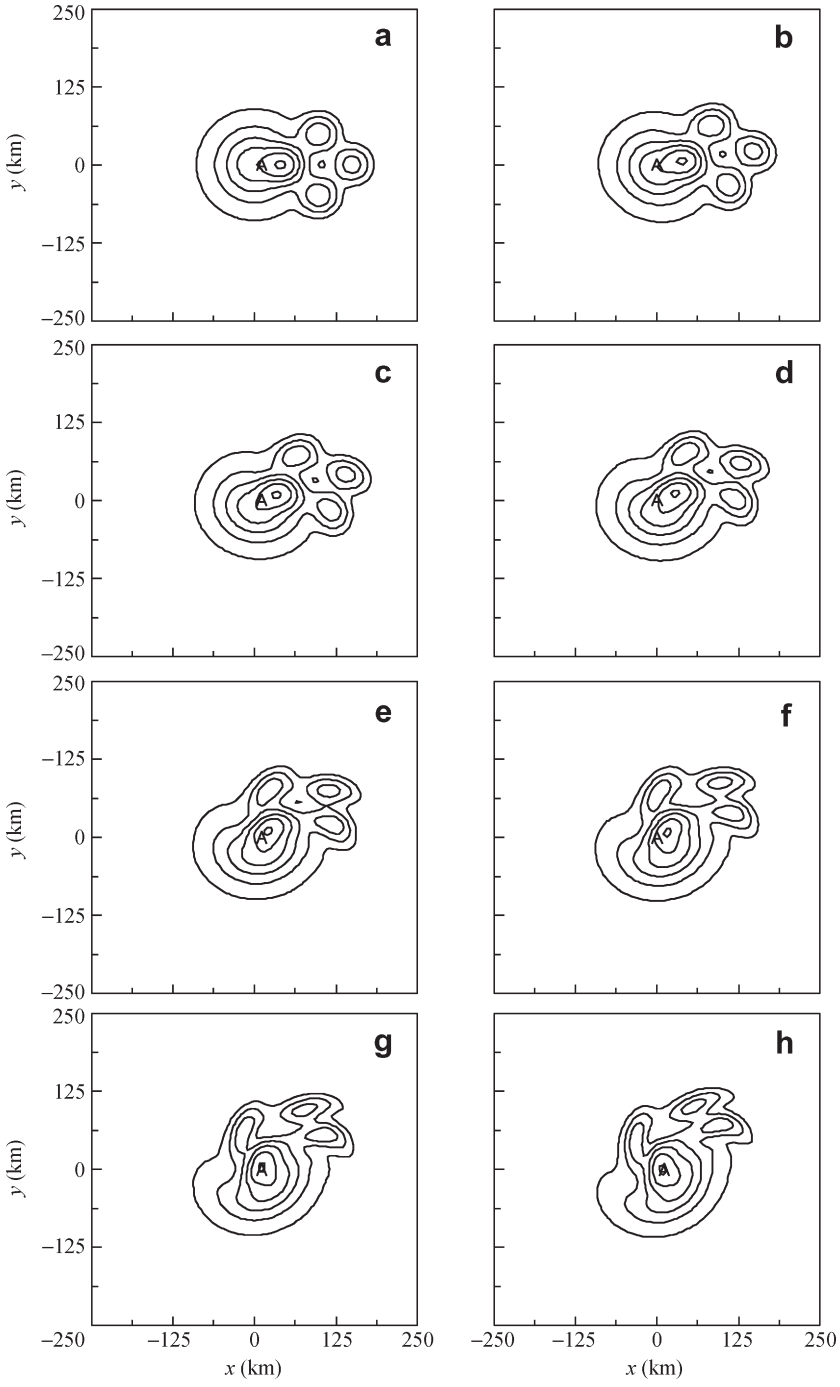

Fig. 1. Hourly evolution of the relative vorticity field in the time period of 0–7 h in EXA without topography. The panel is a 500 km square centered at Letter A, within the computational domain of 2000 km × 2000 km. The contour interval is 0.5×10^{-4} s^{-1}, and the outmost and innermost contours denote 0.5×10^{-4} s^{-1}, 3.0×10^{-4} s^{-1}, respectively. (a) $t = 0$ h; (b) $t = 1$ h; (c) $t = 2$ h; (d) $t = 3$ h; (e) $t = 4$ h; (f) $t = 5$ h; (g) $t = 6$ h; (h) $t = 7$ h.

for the slight reduction of V_{max} in EXA. In contrast to EXA, the dissipative effect resulted from smoothing also exists in EXB, but V_{max} exhibits a remarkable increasing trend due to the incorporation of topographic term (Fig. 5).

3.3. Possible reason for the intensification of the major vortex due to the incorporation of topography

Luo et al. [17] analyzed the effect of topography on the motion of vortex. When there was no terrain present, two meso-β vortices anticlockwise rotated mutually throughout the experiment. In the initial field of the experiment with topography, there were two meso-β vortices over the south edge of topography, and the initial relative vorticity over the central area of topography was zero. After a time period of integration, a negative vorticity lump appeared over the central area due to the constraint of absolute vorticity conservation. In this way, incorporating the topography causes a dramatic change from the "pure" binary vortex mutual rotation

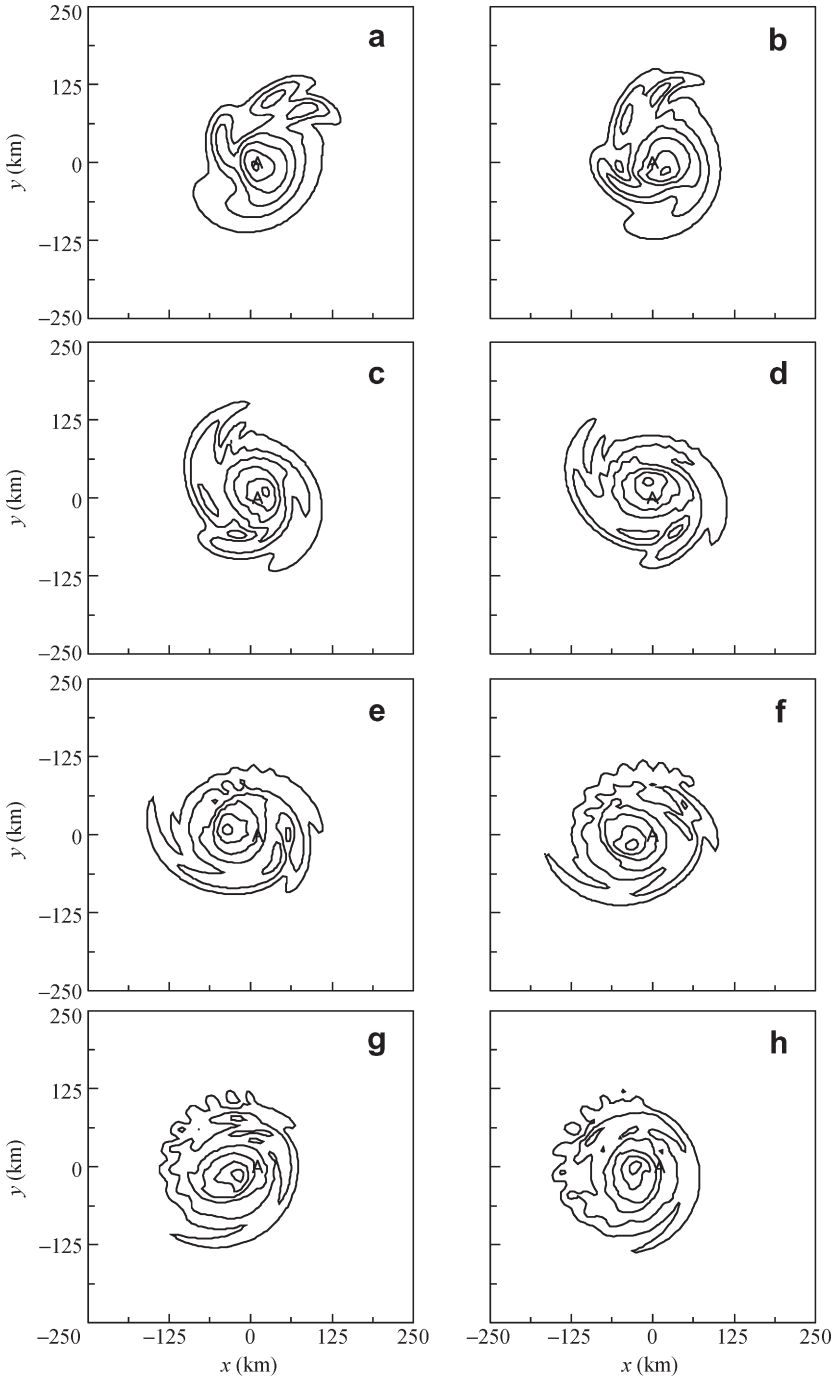

Fig. 2. Four-hourly evolution of the relative vorticity field in the time period of 8–36 h in EXA without topography. The others are the same as Fig. 1. (a) $t = 8$ h; (b) $t = 12$ h; (c) $t = 16$ h; (d) $t = 20$ h; (e) $t = 24$ h; (f) $t = 28$ h; (g) $t = 32$ h; (h) $t = 36$ h.

to a "triple vortex" (two meso-β vortices with positive vorticity and one vorticity lump with negative vorticity) interaction. The quasi-final state flow patterns of the mutual rotation of binary vortex and the interaction among triple vortex were completely different.

In EXB, the center of initial major vortex coincides with the center of underlying topography, and so the initial relative vorticity over the center of topography is not zero. As the time integration goes on, although the negative vorticity lump cannot appear immediately in the central area of topography, the positive vorticity there should reduce. In fact, the relative vorticity at the center of topography VOR_c does reduce, and its value has become negative after 30 h. On the contrary, VOR_c does not change obviously in EXA (Fig. 6).

The reduction of VOR_c or even sign-reversing at the center of topography (i.e. point A of the computational domain) leads to such a consequence that the center of quasi-final state vortex cannot lie in the vicinity of point A, and it also cannot depart far away from point A due

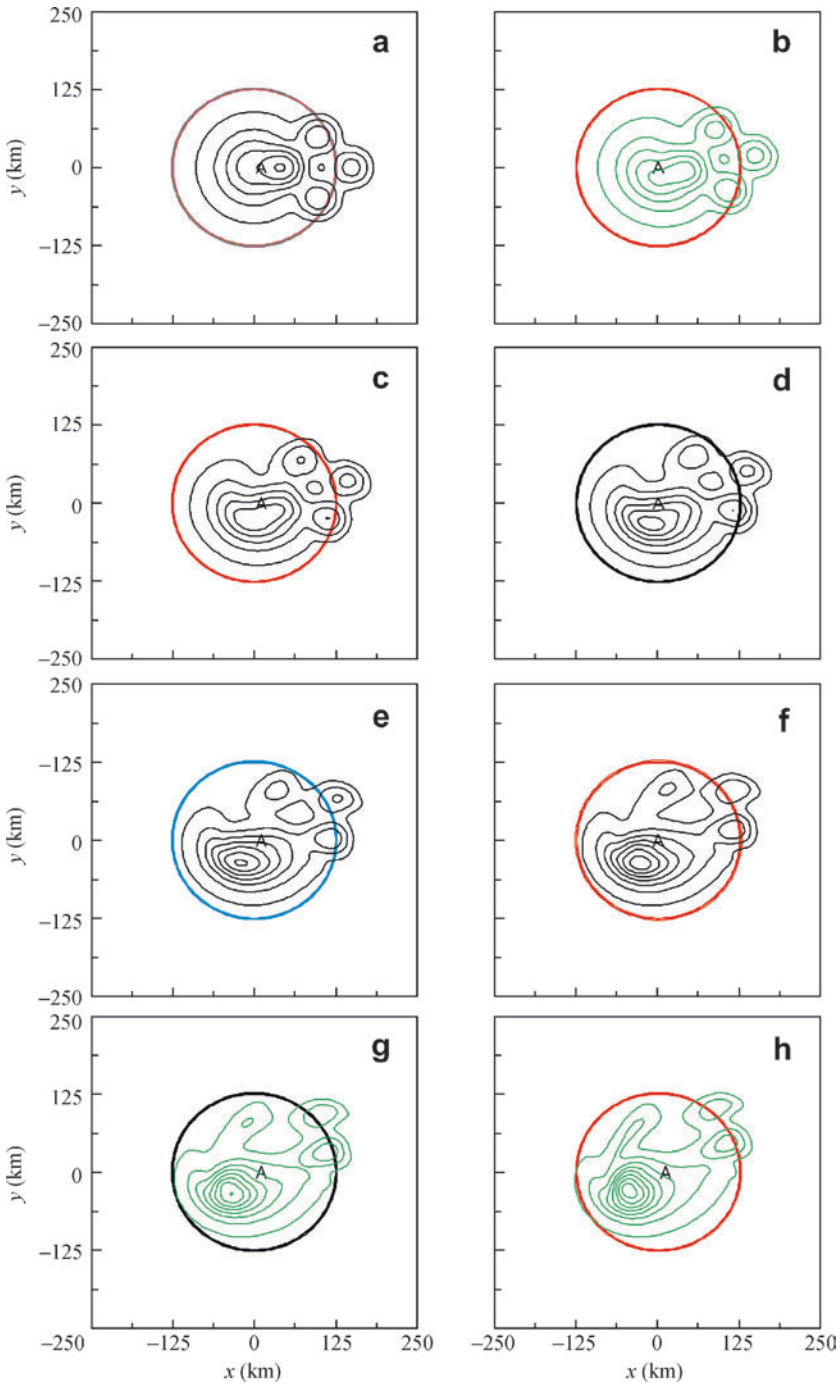

Fig. 3. Hourly evolution of the relative vorticity field in the time period of 0–7 h in EXB with topography. The thick solid line circle approximates the outer edge of the topography, and the others are the same as Fig. 1.

to a weak ambient flow. Therefore, the quasi-final state vortex can only stay on the mountain slope, which results in the reduction of the spatial scale of the vortex (comparing Fig. 2(f)–(h) with Fig. 4(f)–(h)). The total kinetic energy of the model domain W is not affected by the incorporation of topography, and so W in EXA and EXB at $t = 36$ h should be identical. According to the calculation, the relative error $D_w < 0.001$, where $D_w = (W(B) - W(A))/W(A)$, and $W(B)$, and $W(A)$ are the total kinetic energy in EXB and EXA at $t = 36$ h, respectively. The total kinetic energy is almost not changed, but the spatial scale of quasi-final state major vortex is obviously reduced after the incorporation of topography, which must result in the concentration of kinetic energy or energy, i.e. the increase of ξ_{max} and V_{max}. This might be a possible cause for the intensification of the quasi-final state major vortex due to the incorporation of topography.

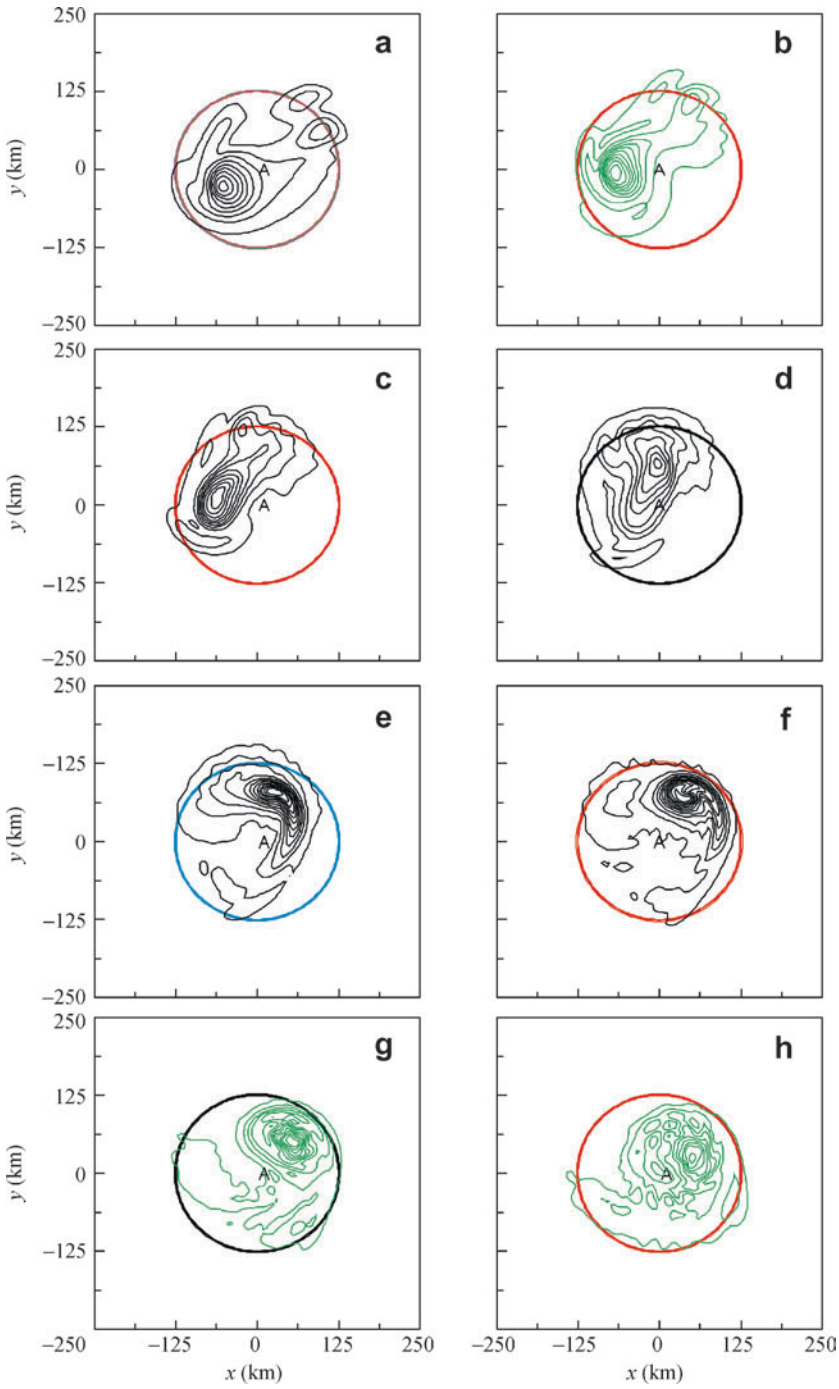

Fig. 4. Four-hourly evolution of the relative vorticity field in the time period of 8–36 h in EXB with topography. The thick solid line circle approximates the outer edge of the topography, and the others are the same as Fig. 2.

4. Conclusions and discussion

Self-organization, complexity, and diversity are characteristic behaviors existing generally in natural world, and have become of interest in many fields. Luo et al. [17] have analyzed the interaction of vortices from a novel viewpoint of self-organization. Luo and Liu [18] have studied the self-organization and complexity of tropical storm. In the actual atmosphere, terrain frequently intensifies the vortex and brings torrential rain disaster. A lot of correlatively observational facts and analysis works have been accumulated and performed, and much progress in studies on the mechanisms has also been achieved. However, to completely understand the mechanisms, much work is required. In view of self-organization, based on the study of Enagonio and Montgomery [12], this paper incorporates the effects of weak ambient flow and topography to analyze the effect of topography on the intensity of self-organized vortex and its possible mechanism. Results show that the topography incurs the intensification of quasi-final state

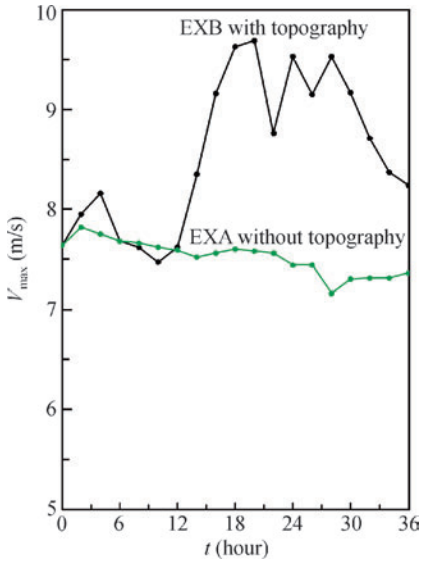

Fig. 5. Temporal evolution of the maximum wind speeds in EXA and EXB.

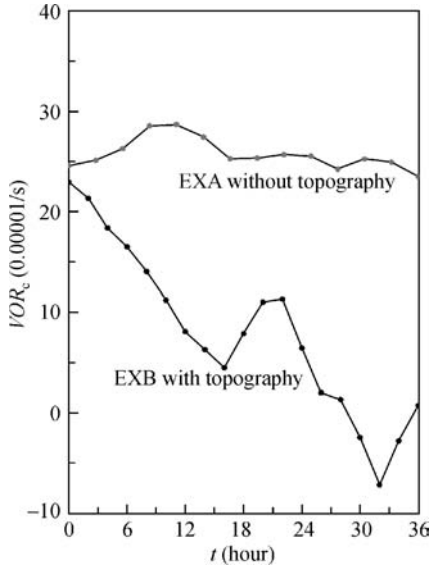

Fig. 6. Temporal evolution of the relative vorticity at the center of the computational domain in EXA and EXB.

vortex. The squeezing of topography against the quasi-final state vortex reduces its spatial range, and on the other hand, the incorporation of topography will not change the total kinetic energy of the model domain. Therefore, the reduction of the spatial range of the vortex directly results in the concentration of energy, and the increases in the relative vorticity of the quasi-final state vortex and in the local maximum wind speed. This is a possible mechanism obtained from the point of view of self-organization.

When a vortex approaches a mesoscale topography in the atmosphere, it is possibly useful to look at the evolution of the spatial scale of the vortex and to identify whether the vortex can intensify.

There are many other possible factors determining the intensification of vortex, such as the heating of latent heat produced by vigorous convection, on which further studies are needed.

Acknowledgement

This work was supported by National Natural Science Foundation of China (Grant No. 40775038).

References

[1] Chen LS, Ding YH. The Conspectus of Western Pacific Typhoon (in Chinese). Beijing: Science Press; 1979, [491].
[2] Mong ZY, Xu XD, Chen LS. The impact mechanism of the secondary circulation system induced by Taiwan Island orography on the anomalous track of typhoon motion. Chin J Atmos Sci 1998;22:156–68.
[3] Chen LS, Xu XD, Luo ZX, et al. An Introduction to Tropical Cyclone Dynamics (in Chinese). Beijing: China Meteorological Press; 2002, [317].
[4] Luo ZX, Chen LS. A study on the influence of terrain on vortex Rossby wave. Prog Nat Sci 2003;13:372–7.
[5] Kuo HC, Williams RT, Chen JH. Topographic effects on barotropic vortex motion: no mean flow. J Atmos Sci 2001;58:1310–27.
[6] Luo ZX, Chen LS. Effect of Taiwan Island orography on the track of typhoon motion. Scientia Atmospherica Sinica (in Chinese) 1995;19:701–6.
[7] Yeh TC, Elsberry RL. Interaction of typhoon with the Taiwan orography. Part I: upstream track deflections. Mon Wea Rev 1993;121:3193–208.
[8] Smolarkiewice PK, Rotunno R. Further results on lee vortices in low-Froude-number flow. J Atmos Sci 1991;48:2204–11.
[9] Gao ST, Chen H. The study of the lee wave passing over large topographies. Acta Meteorologica Sinica (in Chinese) 2000;6:654–65.
[10] Gao ST, Ping F. Laboratory studies of a stratified rotating flow past an isolated obstacle. Chin Phys Lett 2003;20(7):1094–7.
[11] Gao ST, Ping F. An experiment study of lee vortex with large topography forcing. Chin Sci Bull 2005;50(3):248–55.
[12] Enagonio J, Montgomery MT. Tropical cyclogenesis via convectively forced vortex Rossby waves in a shallow water primitive equation model. J Atmos Sci 2001;58:685–705.
[13] Luo Z, Liu C. An investigation into axisymmetrixation of a vortex embedded in horizontal shearing currents. J Geophys Res 2007;12:D06103.
[14] Evans JL, Holland GJ, Elsberry RL. Interactions between a barotropical vortex an idealized subtropical ridge, Part 1: Vortex motion. J Atmos Sci 1991;48:301–14.
[15] DeMaria M. Tropical cyclone motion in a no divergent barotropical model. Mon Wea Rev 1985;113:1199–210.
[16] Gray WM. The formation of tropical cyclones. Meteor Atmos Phys 1998;67:37–69.
[17] Luo ZX, Zhou XJ, Gao ST. Two type possible mechanisms for vortex self-organization. Sci China (Ser D) 2006;36:201–8.
[18] Luo Z, Liu C. A tropical storm: self-organization and complexity. Geophys Res Lett 2007;34:L05802.